water

MDPI

Article

Shrinking Desert Channel Response to Increasing Human Interferences and Changing Natural Factors in the Upper Yellow River

Yongshan Li [1,2], Xiaopeng Jia [3,*], Haibing Wang [4], Jian Wang [1] and Qimin Ma [5]

1 School of City and Planning, Yancheng Teachers University, No. 2 Xiwangdadao South Road, Yancheng 224007, China; liys@yctu.edu.cn (Y.L.); wjshuigong@163.com (J.W.)
2 North Jiangsu Institute of Agricultural and Rural Modernization, Yancheng Teachers University, Yancheng 224007, China
3 Key Laboratory of Desert and Desertification, Northwest Institute of Eco-Environment and Resources, Chinese Academy of Sciences, No. 320th Donggang West Road, Lanzhou 730000, China
4 College of Desert Control Science and Engineering, Inner Mongolia Agricultural University, No. 29 Ordos East Street, Hohhot 010011, China; hbwang@imau.edu.cn
5 College of Resources and Environment, Chengdu University of Information Technology, Chengdu 610225, China; mqm@cuit.edu.cn
* Correspondence: jiaxp@lzb.ac.cn

Abstract: Many rivers are tightly coupled and intersected with aeolian sand dunes, whose geomorphological evolution involves not only fluvial processes but also aeolian processes that pose a new challenge to fluvial geomorphological studies. However, due to few field studies, our overall understanding of the desert channel geomorphic process is limited. In this paper, we present an outstanding example of desert river channel evolution regulated by aeolian–fluvial interactions in the Ulan Buh Desert of the Yellow River, based on a long time series data set (1966–2019) of channel cross-sections. The results indicate that the lateral addition of aeolian sand, the water–sediment relationship and human interference have a significant role at different periods of channel evolution. Before 1986, higher discharge, lower sediment content and greater intensity of aeolian activity caused aeolian–fluvial interactions and a relative scouring and silting balance in the channel, with little human activity. From 1986 to 2000, an increase in large reservoir operation, vegetation coverage and floodplain farming, coupled with water–sediment relationship variation, caused rapid deposition and shrinkage of the river channel. From 2000 to 2014, the channel kept a slight scouring state. With Haibowan reservoir operation beginning in 2014, the talweg experienced rapid scouring and undercut rebound. However, an expanding and stable floodplain accelerated sedimentation on the floodplain and weakened river lateral erosion, indicating that the channel has shown a shrinkage trend. Meanwhile, wavelet analysis results indicate that human interferences and aeolian activities have no significant role in the periodical characteristics of the channel's longitudinal erosion and deposition. Therefore, on the whole, increasing human interferences and decreasing wind dynamics have driven this desert wandering channel to be stable, and to gradually form a new balance between erosion and sedimentation.

Keywords: Ulan Buh Desert; desert river; Yellow River

check for updates

Citation: Li, Y.; Jia, X.; Wang, H.; Wang, J.; Ma, Q. Shrinking Desert Channel Response to Increasing Human Interferences and Changing Natural Factors in the Upper Yellow River. *Water* **2023**, *15*, 4226. https://doi.org/10.3390/w15244226

Academic Editors: Hongshan Gao, Yaling Chen and Yuanxu Ma

Received: 8 November 2023
Revised: 28 November 2023
Accepted: 5 December 2023
Published: 8 December 2023

1. Introduction

Channel geomorphological changes are usually complex in alluvial sandy-bed rivers, driven by the interactions of multiple factors, such as flow conditions, suspended sediment content and bedload composition and characteristics, of which a more comprehensive understanding has been recognized over the past half century [1–19]. However, in arid and semi-arid regions, all kinds of aeolian sand dunes are the most common landforms and landscapes, e.g., [1,20–24], where many rivers are tightly coupled and intersected with aeolian sand dunes [25–31]. The geomorphological evolution of these involves not only fluvial processes but also aeolian processes that pose a new challenge to fluvial geomorphological studies. This has attracted more interest around the world and has been gradually recognized by geomorphologists [23,24,31–34], promoting an increasing understanding of aeolian–fluvial interaction in arid and semi-arid zones for nearly two decades. It is key for channel evolution in alluvial desert rivers that abundant aeolian sediments are input into riverbeds, disrupting normal fluvial processes, easily causing channel silting, narrowing channel paths, diverting flow and even damming rivers, further threatening local human activity. Thus, we need to further understand the response characteristics of the alluvial desert river channel to aeolian activities and human interference, revealing the desert river channel evolution mechanism and direction which can support the ecological restoration, development and management of riverbanks.

In these desert rivers, the transformation of the dominant geomorphic agency from wind to flowing water leads to complexity and uncertainty in the evolution of erosion and the deposition of desert rivers. Some studies have identified that, in addition to flow conditions and sediment loads, the lateral infusion of aeolian sand into riverbeds also plays a significant role in desert river channel changes. Smith and Smith [33] and Li et al. [35] indicate that alluvial rivers with low gradients that flow across aeolian dunes lead to abrupt additions of sandy bedload caused by large lateral inputs of aeolian sand, causing channel widening and braiding. Jia et al. [36] proposed that in ephemeral desert rivers with a large gradient, aeolian processes can move dunes and narrow the channels in the dry season, but storm floods can cause the hyper-erosion of dune-covered banks and widen the channels, inducing hyper-suspended sediment concentration flows during the flood season. However, these few field studies limit our overall understanding of this desert channel geomorphic process.

The Yellow River flows across Ulan Buh Desert dune fields in the upper reaches, similarly to the lower reaches, with high sediment content, suspended river and flood threats, and has developed a large, unstable, braided-wandering sandy bed. However, it is uniquely characterized by a large lateral addition of aeolian sand that constitutes coarser bedloads distinguishable from fluvial sediment upstream and two grain size fractions separately transporting and depositing [37,38]. Ta, Wang and Jia [32] documented that the decreasing flow discharge and accumulation of lateral coarse sediment supply (>0.08 mm median grain size) from wind-borne sediments coarsened the channel bed surface locally, leading to the channel aggradation rate accelerating rapidly, which were also verified heavy mineral and element indicators [39,40]. However, with the increasing human interference of bank ecological restoration along the Ulan Buh Desert Reach of the Yellow River and the Haibowan reservoir operation, the environment of the lateral infusion of aeolian sand into the Yellow River is changing gradually. Recently, there have been some new channel changes and characteristics that need to be evaluated within a longer time scale to reveal the mechanism of desert river evolution and trends in response to human interference and changing natural factors. Here, based on a long time series data set (1966–2019) of channel cross-sections in the Ulan Buh Desert of the Yellow River, combined meteo-hydrological data and NDVI data, our objective is to clarify the desert river channel evolution characteristics, processes and causes in response to increasing human interference and changing natural factors.

2. Study Area

The Ulan Buh Desert reach is located in the ending reaches of the Upper Yellow River, which flows northward through the Ulan Buh dune fields at its east margin, starting at the Haibowan reservoir (operated in 2014) and ending at the Bayangaole gauging station, with a total channel length of 88 km. The desert reach intersects sand dunes (Figure 1) with small ephemeral tributary rivers along the right bank. The study area is located in the East Asian monsoon region edge and belongs to a temperate continental semi-arid climate. The predominant wind directions of NW (north-west wind), W (west wind) and

WS (west-south wind) in the winter and spring transport large volumes of aeolian sand from the desert toward the river, causing a large lateral infusion of sand dunes in this desert riverbed. It is confirmed that this reach has developed a large sandy bed of which the bedloads consist of coarser sediments (>0.08 mm) mainly sourced from the Ulan Buh Desert [32,41]. The Yellow River water level is higher than the low land on the left bank, developing a secondary suspended river, characterized by a typical braided and wandering alluvial channel, with a very low gradient of 0.14‰ and high sediment content, similar to the lower channel of the Yellow River.

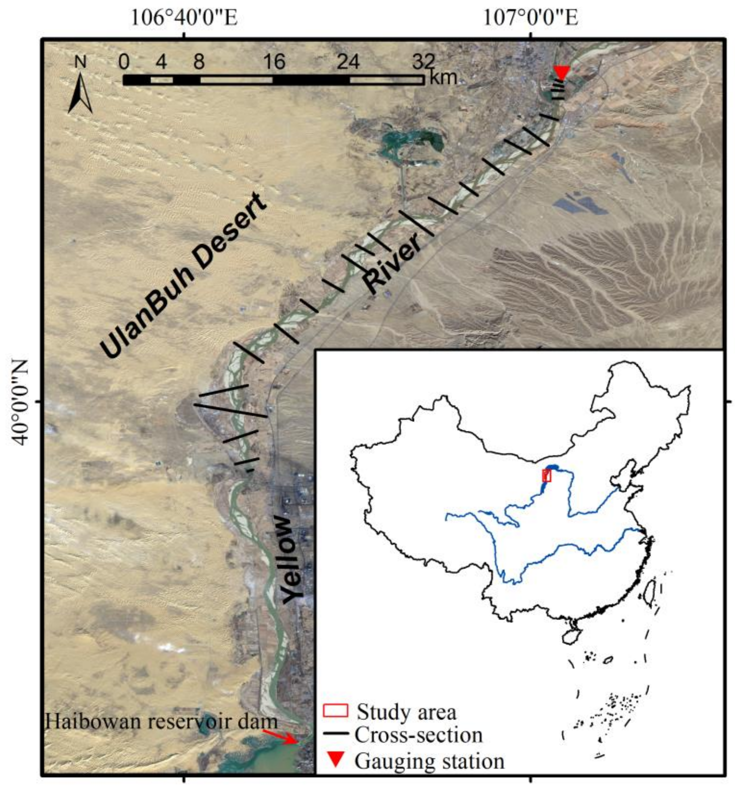

Figure 1. The Ulan Buh Desert reaches of Yellow River and channel cross-section distribution.

3. Data and Methods

3.1. Data

We collected a data set of a total of 23 channel cross-sections, with intervals of about 2~5 km on average (Figure 1), measured annually in April and October, for 54 years (from 1966 to 2019) in the Ulan Buh Desert reach. We also collected hydrological data, supported by the Yellow River Engineering and Management Bureau of the Inner Mongolia Autonomous Region. Meteorological data are from the China Meteorological Data Sharing Service System (http://data.cma.cn/, accessed on 14 August 2020). NDVI data are from the China Annual Vegetation Index (NDVI) and the spatial distribution data set is from the registration and publication system of resources and environmental science data (http://www.resdc.cn/DOI/, accessed on 27 May 2022) [42], with a spatial resolution of 1 km.

3.2. Methods

3.2.1. Mann–Kendall Test

The nonparametric Mann–Kendall (M-K) test method, developed by Mann (1945) [43] and Kendall (1948) [44], was used to detect significant long-term trends in different variables of river channels from 1966 to 2019 in the Ulan Buh Desert reach of the Yellow River.

3.2.2. Wavelet Analysis

The wavelet analysis method is based on the time-domain analysis method, which is widely used in hydrology, meteorology and other disciplines [45]. The lateral scouring and silting process of the river channel is a direct response to wind-blown sand, water and sediment. This paper attempts to reveal the periodic change characteristics of the lateral scouring and silting swing of the river channel based on the wavelet analysis theory. For a given wavelet function $\psi(t)$, the continuous wavelet transformation of the time series is $f(t)$, and the continuous wavelet transformation is:

$$W_f\ (a,\ b)\ = |a| - \frac{1}{2}\int_{-\infty}^{\infty} f(t)\overline{\psi}(\frac{t-b}{a})dt \tag{1}$$

where a is the scale factor ($a \neq 0$), reflecting the frequency domain characteristics; b is a time factor, reflecting the complex conjugate function of overlay $\overline{\psi}(\frac{t-b}{a})dt$.

Here, the Morlet complex wavelet function is selected to analyze the change period of lateral scouring and silting oscillation. At first, the intensity sequence of the transverse oscillation of the talweg points in the river channel is standardized, then it is extended to weaken the "boundary effect" at both ends of the sequence and then the wavelet transformation is performed.

3.2.3. Estimation of Erosion and Sedimentation

The calculation of river channel erosion and deposition is based on the large section of the river channel. Kasai et al. [46] proposed a section-based calculation method for river channel erosion and deposition (Formulas (1) and (2)). Research shows that the calculated erosion and deposition amount of this method has good reliability and applicability [47]. In the scouring and silting amount calculation method proposed by Kasai et al., the distance between sections is the distance between the middle points of the river width lines of two adjacent sections. The error is relatively small when the width of the river channel between sections changes little and the distance between sections is close. However, greater variation of the river width between the two sections will cause greater errors. In such cases, the distance between the sections (L_k) is treated as follows:

First, the polygon of every two adjacent cross-sections and the bank floodplain boundary are constructed to calculate the area of each polygon (Figure 2). Then, the average width of the two sections is calculated and the polygon area is divided by the average width of the two sections to obtain the distance between the two sections. Finally, it is brought into Kasai's calculation formula and the appropriate sediment unit weight is selected (according to the drilling data of wind, sand and beach sediment, here ρ takes about 1.6 t·m^{-3}) to calculate the amount of channel sediment erosion and deposition.

The calculation method of channel erosion and deposition is as follows:

$$V_k = \frac{1}{3}(A_i\ +\ A_{i+1}\ +\ \sqrt{A_i A_{i+1}}) \times L_k \tag{2}$$

$$S = \rho \sum V_k \tag{3}$$

$$L_k = \frac{P_k}{\frac{1}{2}(w_i + w_{i+1})} \tag{4}$$

where ρ is the unit weight of the sediment (unit: t·m^{-3}); P_k is the constructed polygon area; L_k is the distance between the two cross-sections (unit: m); S is the siltation amount (unit: t); V_k is the volume between the two cross-sections (unit: m^3); w_i is the cross-section width; A_i is the cross-section area (unit: m^2).

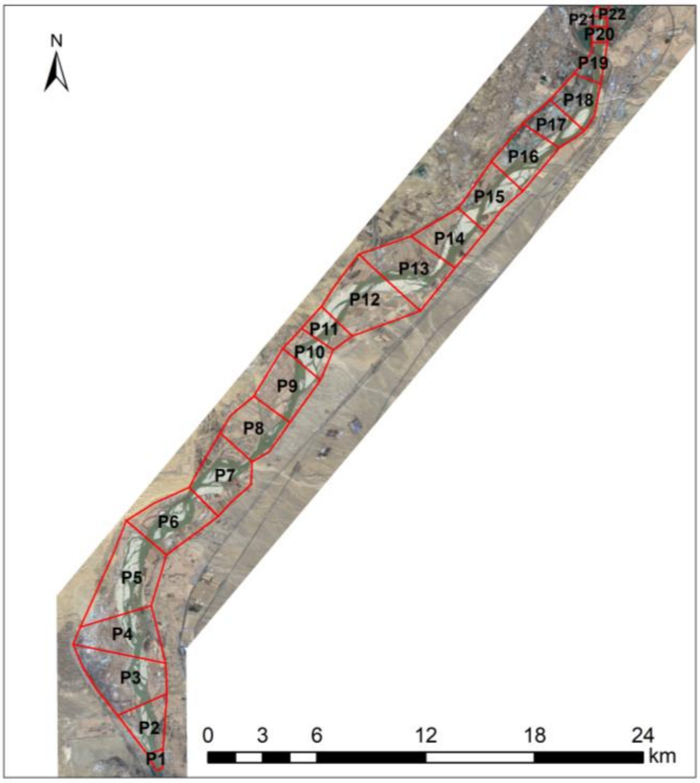

Figure 2. Illustration of polygon construction of every two adjacent cross-sections and the bank floodplain boundary.

4. Results

4.1. Channel Scouring–Silting Annual Changes

4.1.1. Talweg

Based on changes in talweg elevation and scouring–depositing variation during the flood season and the dry season, respectively, combined with a large reservoir operation time joint, five periods were divided from 1966 to 2019 (Figure 3). Figure 4 indicates that from 1966 to 1975, the riverbed showed a slight scouring state, however, with a significant scouring–depositing differentiation in the flood period and dry period, respectively. From 1975 to 1986, the riverbed talweg elevation showed a slight depositing trend, partly induced by an increasingly large reservoir operation upstream and gradual changes in the water–sediment relationship that caused channel aggradation, partly because of the lateral infusion of bank aeolian sand into the riverbed that was not easily transported by flow. Then, from 1986 to 2000, an abrupt increase in SSC (suspended sediment concentration) release from the Qingtongxia reservoir induced a rapid aggradation process and the talweg elevation in 2000 was 1.5 m higher than that in 1966. From 2000 to 2014, the riverbed talweg elevation began to self-regulate scouring; by 2014, the riverbed elevation was scoured to the same elevation as in 1966. In the aggradation period, the channel presented a significant scouring–depositing differentiation in the dry period and the flood period, respectively, of which talweg aggradation dominated in the flood season, mainly owing to high SSC and lateral infusion of aeolian sands. After 2014, with Haibowan reservoir operation, scouring downstream from the dam led to rapid riverbed scouring and undercutting both in the flood season and the dry season. The talweg elevation in 2019 was 1.5 m lower than that in 1966.

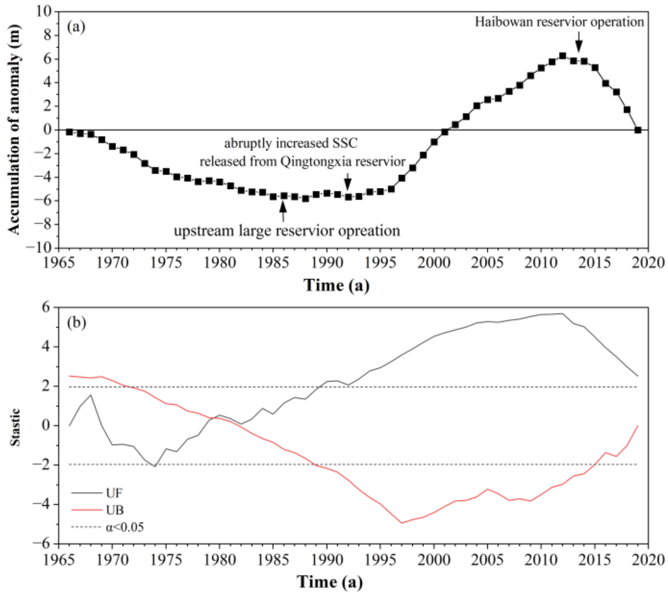

Figure 3. Talweg elevation (**a**) accumulation of anomaly and (**b**) M-K test value from 1966 to 2019.

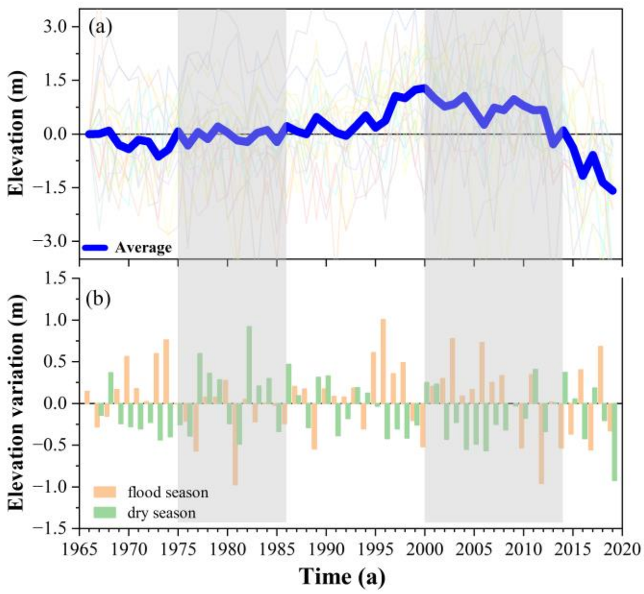

Figure 4. Changes of (**a**) talweg elevation based on the elevation in April 1966 and (**b**) talweg elevation scouring and depositing variation during the flood season and dry season.

4.1.2. Channel Cross-Section Area

The changes and tendencies in channel cross-section area are similar to that of the talweg from 1966 to 2019 (Figures 5 and 6), but different in details. From 1966 to 1985, the channel cross-section area kept a relatively balanced, stable state. However, there was a rapid and abrupt decline from 1986 to 2002 and then a stable period in 2003–2013. After 2014, the channel cross-section area rapidly scoured but did not return to the state of 1966, which is different from talweg changes. From the perspective of seasonal variation, the channel cross-section shows a scouring and silting differentiation in the flood season and the dry season from 1966 to 2014, respectively, which illustrates that the channel cross-section area increased in the dry season, while it declined in the flood season. This differentiation indicates that channel aggradation is induced in the flood season while scouring is induced in the dry season. However, from 2014 to 2019, the trend of silting in the flood season gradually weakened and the channel cross-section area rapidly enlarged, probably in response to the scouring effect of the Haibowan reservoir operation. Compared to talweg changes, we found that the response speed of talweg scouring and silting to flow is faster than that of the channel cross-section area, but not sensitive seasonally, while channel cross-section scouring and silting differentiation in the flood season and the dry season is clear.

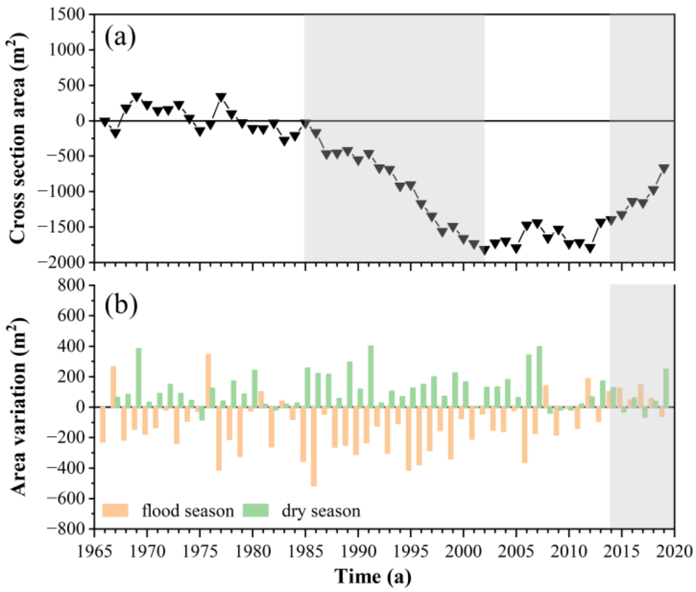

Figure 5. Changes in (**a**) relative channel cross-section area based on the cross-area in April 1966 and (**b**) its variation between flood season and dry period from 1966 to 2019.

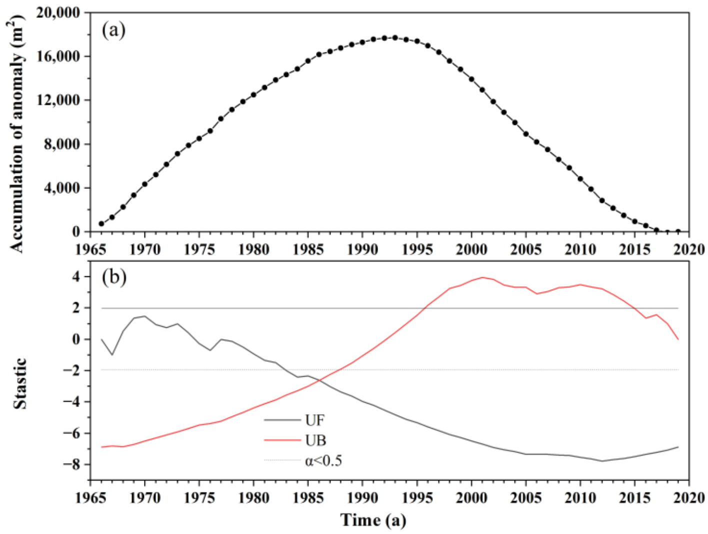

Figure 6. Channel cross-section area (**a**) accumulation of anomaly and (**b**) M-K test from 1966 to 2019.

In detail, the channel cross-section area changes do not completely correspond to the talweg changes from 1966 to 2019. Before 1986, talweg scouring and undercutting were accompanied by slight channel cross-section shrinkage; then, there was a synchronous rapid silting change both in the talweg and cross-section from 1986 to 2013. However, a turning point of talweg elevation change occurred in 2014, after the talweg undercut rapidly, whose elevation was lower than that in 1966. Although the channel cross-section presented a scouring state, there was a slow decrease rate in the cross-section area. These changes were probably caused by an increasing and stable floodplain that accelerated sedimentation on the floodplain and weakened the river's lateral erosion.

4.1.3. Scouring–Deposition Amount

Based on the channel cross-section and the bank floodplain boundary extracted from RS images (Figure 2), the channel scouring and deposition amounts were estimated from 1966 to 2019 (Figure 7). Similarly to the river cross-section area changes, the channel kept a relatively balanced and stable state in the first 20 years. However, after 1986, due to the Longyangxia and Liujiaxia reservoir joint operation, there was rapid silting at 20×10^4 t·a^{-1}·km^{-1} from 1986 to 2003; then, it kept a stable period in 2003–2013; after 2014, the channel rapidly scoured but did not return to the state of 1966. From the perspective of seasonal variation, the channel cross-section showed a scouring and silting differentiation in the flood season and in the dry season from 1966 to 2013, respectively, which illustrates that the channel cross-section area increased in the dry season while declining in the flood season. This differentiation indicates that channel aggradation was induced in the flood season, while scouring occurred in the dry season. After 2014, the trend of silting in the flood season gradually weakened and the channel cross-section enlarged, probably in response to the scouring effect of the Haibowan reservoir operation. However, the deposition amount and the scouring rate were similar to the cross-section area change, which was slower than the talweg undercut.

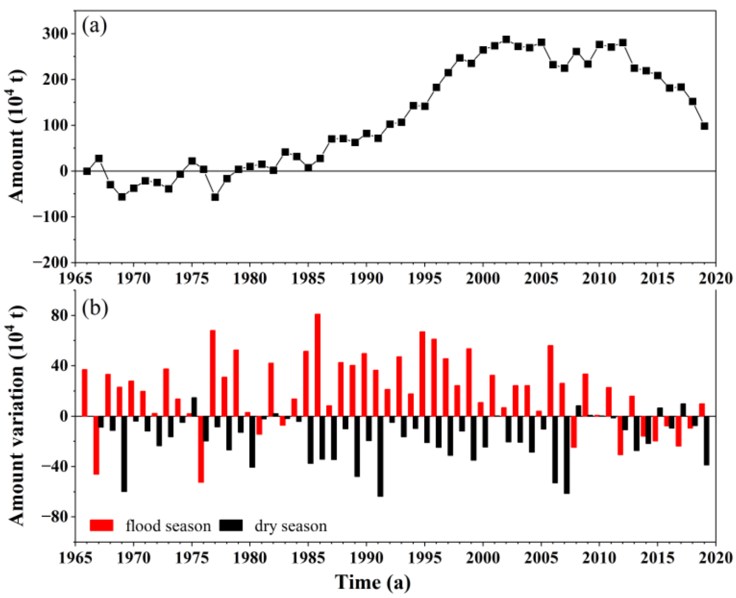

Figure 7. Changes of (**a**) deposition amount per kilometer and (**b**) its variation between flood season and dry period from 1966 to 2019.

4.2. Evolution Cycle of Scouring–Depositing

Wavelet analysis shows that there were obvious periodical changes in the longitudinal scouring and deposition of the river channel from 1966 to 2019 (Figure 8). The results show that during the research period from 1966 to 2019 there was a periodic change under a single characteristic time scale in the longitudinal scouring and silting evolution process of the braided channel in the wide valley of the Ulan Buh Desert of the Yellow River. That is, the periodic adjustment rule of riverbed scouring and silting under the 32–64a characteristic time scale is significant, and it is global. Correspondingly, the time scale of 53a and 52a in the wavelet variance chart corresponds to the maximum peak value of the talweg and the cross-section area, respectively, which indicates that the longitudinal scouring and silting cycle of the riverbed at the characteristic time scale of 52a–53a changed most significantly (Figure 9). The riverbed underwent 1.5 periodic scouring and silting adjustments in the study period, with an average scouring and silting cycle of 36 years. Thus, these findings indicate that increasing human interference, and decreasing aeolian activities have no significant role in the periodical characteristics of the channel's longitudinal scouring and deposition.

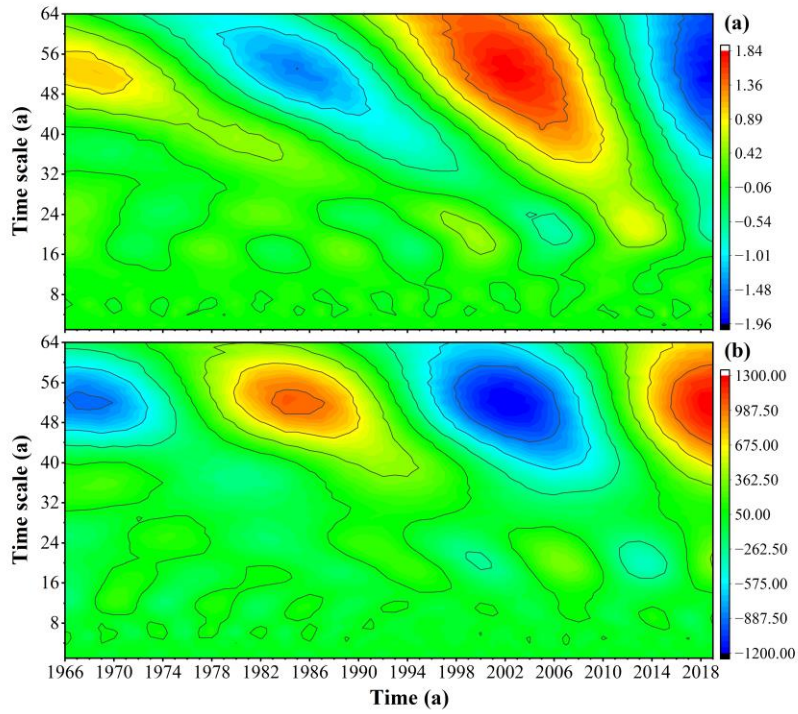

Figure 8. Talweg (**a**) and cross-section (**b**) wavelet coefficient real-time contour plot and wavelet variance plot.

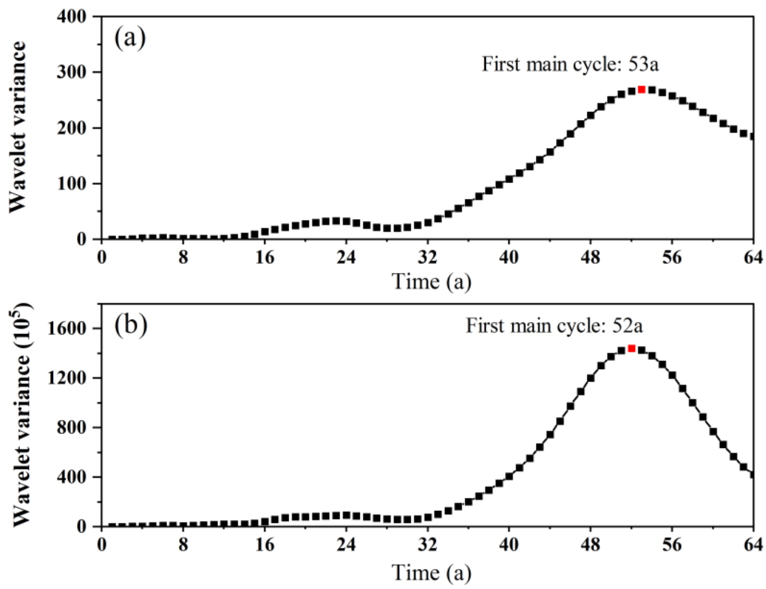

Figure 9. Talweg (**a**) and cross-section (**b**) wavelet variance plot.

4.3. Bedload Grain Size Changes

Riverbed surface loads were sampled in April and October, respectively, accompanied by the channel cross-section surveyed in each year, whose grain size characteristics can reflect sediments sources and flow dynamics, indicating channel erosion and deposition change. Firstly, although this reach is located in the upper river, the bedload grain sizes show that the desert channel developed a typical sandy bed affected by bank aeolian sand [32]. From 1965 to 1988, the bedload grain sizes kept a stable state of approximately 0.125 mm (Figure 10). Then, the bedload grain sizes showed a rapid fining period from 1990 to 2003, responding to rapid channel silting both in the talweg and the channel cross-section in the same period, which were driven by the water–sediment relationship of low-discharge and high-suspended sediment content. After 2003, the bedload grain sizes underwent a rebound near 0.1 mm. Meanwhile, there was also a bedload grain sizing differentiation in the flood period and the dry period accompanied by talweg and channel aggradation in the flood period and scouring in the dry season.

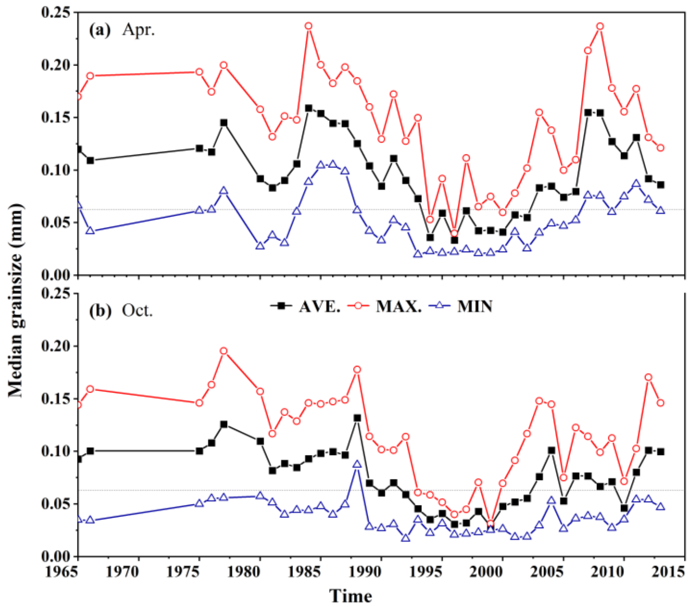

Figure 10. Changes in bedload grain size at (**a**) April and (**b**) October from 1966 to 2013.

5. Discussions

5.1. Relationship between Talweg and River Cross-Section Area

In this desert reach, there was a changing relationship between talweg elevation and channel cross-section with changing influence factors from 1966 to 2019. Although the correlation between talweg elevation and channel cross-section area was significantly negative, Figure 11 showed that the slope of linear regression analysis obviously changed since 2013. After 2013, changes in the amplitude and speed of talweg scouring and deposition were more than that of the channel cross-section area, which indicate that the floodplain had gradually stabilized and expanded, partly because of the increasing NDVI (Figure 12) and the dyke–dam, on the one hand, and the low-discharge flow condition and decreasing aeolian lateral infusion that weakened the sediment lateral transportation process between the riverbed and the aeolian dunes in the floodplain, on the other hand.

5.2. Bank Ecological Restoration

The Ulan Buh Desert, covering an area of only 10,000 square kilometers, is dominated by aeolian dunes. Moving dunes, which make up 37% of the total area, are distributed in the southeast and are intersected by the Yellow River. Lateral infusion of aeolian sand into the riverbed is controlled by, in addition to river lateral erosion and wind–sand dynamic conditions, the vegetation conditions of the underlying surface of the Ulan Buh Desert. In recent decades there was an increase in human activity, such as building grass grids along traffic lines, vegetation restoration and farming on the river floodplain, which induced an increase in vegetation coverage, expanding and stabilizing the floodplain and reducing the lateral infusion of aeolian sand into the riverbed. Figure 12 shows that the NDVI index increased by nearly 0.20 from 1998 to 2019, which was especially contributed to by the left riverbank of the Yellow River. Combined with the decreasing wind speed

(Figure 13), it is obvious that the environment of the lateral infusion of aeolian sand into the river has changed. Where channel lateral scouring is decreasing, the desert channel shows a shrinking trend, which indicates that the influence of the aeolian process on the development and the evolution of the river's geomorphology is gradually weakening.

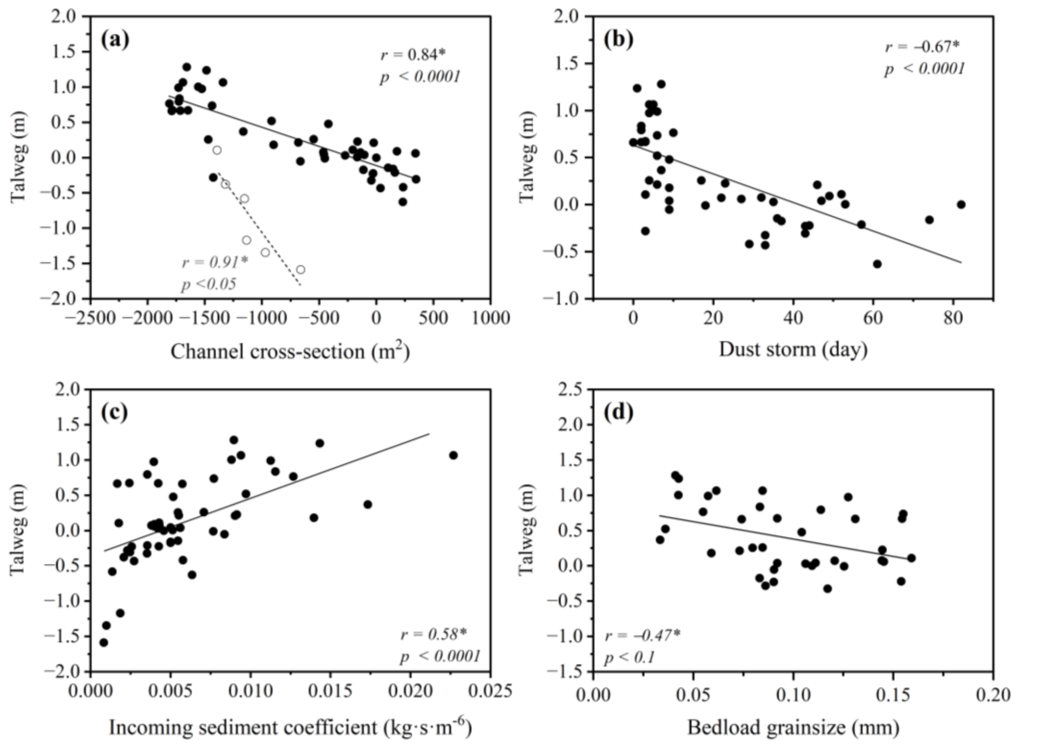

Figure 11. Relationship between talweg elevation and (**a**) channel cross-section area, (**b**) dust storm days, (**c**) incoming sediment coefficient and (**d**) bedload grain size (* correlation is significant at the 0.05 level).

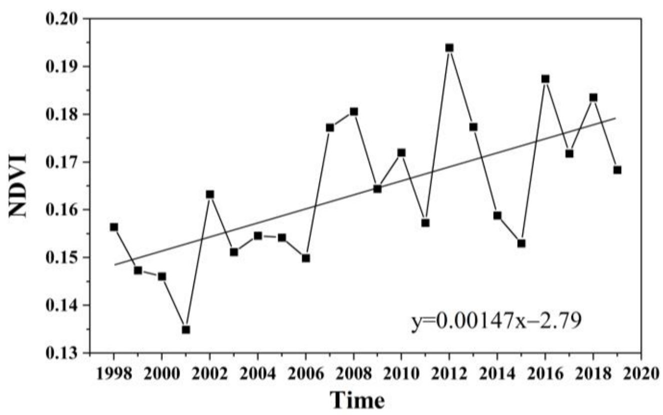

Figure 12. Increased NDVI value of the Ulan Buh Desert from 1998 to 2019 in response to increased human ecological restoration and warm–wet climate change trends.

5.3. Aeolian and Fluvial Factors

Channel changes are complex and are usually regulated by fluvial processes including discharge, suspended sediment characteristics and bed and bank materials. The Yellow River is characterized by high sediment content, and channel change is sensitive to the response of incoordination between water and sediment. In the upstream of the Yellow River there has been a warm and humid trend during the past half century. Figures 13 and 14 show that precipitation presents an ascending trend, whilst runoff does not increase, indicating an obvious decreasing trend after 1986, mainly due to large reservoir operations to account for the increasing human need for irrigation, industrial activities and ecological restoration, partly because of continuous temperature rise that increased evaporation.

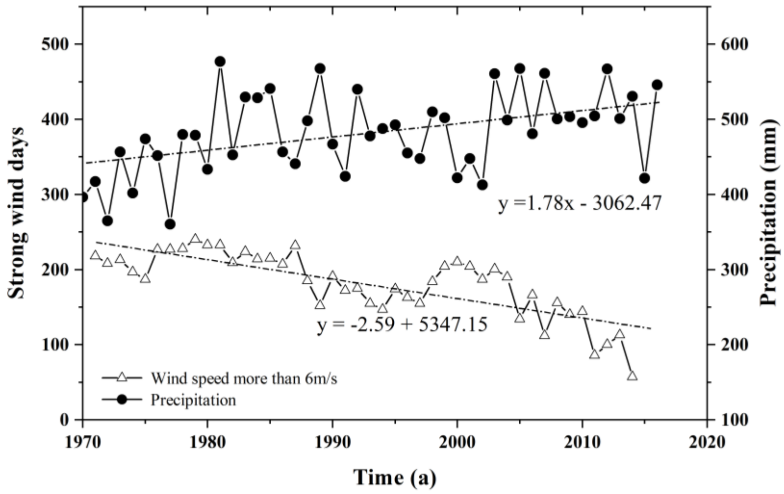

Figure 13. Increased precipitation (16 stations distributed in the upstream of the Yellow River) and decreased strong-wind days at Dengkou station.

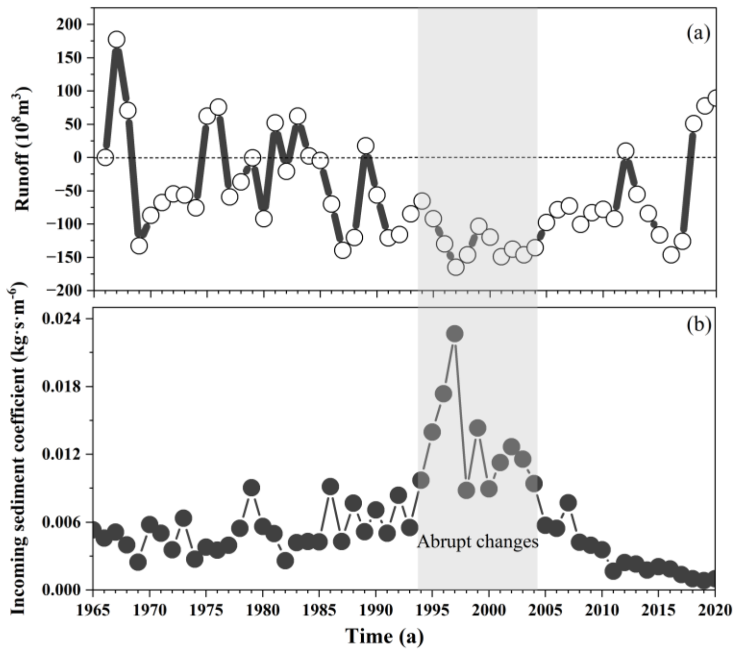

Figure 14. Changes in (**a**) annual runoff and (**b**) incoming sediment coefficient at Bayangaole hydrological station from 1965 to 2020.

In these aeolian–fluvial interaction areas, the lateral infusion of aeolian sand into the riverbed has been found to play a significant role in desert river channel evolution, in addition to flow conditions and sediment loads, which is gradually being supported by the results [33]. Previous research estimated [38] that aeolian sands were eroded and transported into the Yellow River at a rate of approximately 20 million tons every year during the 1970s–1980s, which has been verified and traced using field monitoring data, grain size and heavy mineral and geochemical element evidence. A large amount of wind-blown sand, the grain size of which is more than 0.063 mm, becomes the bedload component and is different from fluvial suspend sediments, the grain size of which is less than 0.063 mm. These coarser sediment bedloads are not transported by normal flow conditions, easily causing channel braiding, frequent lateral shifting and aggradation. The results also indicate that the correlation between talweg elevation and bedload grain size is significantly negative (Figure 11b,d). Figure 13 shows that wind speed had a decreasing trend from the 1970s to the 2010s, which indicates that the decreasing aeolian processes caused a gradual reduction in the lateral addition of aeolian sand into the riverbed. From 1994 to 2004, there was no significant or abrupt reduction in aeolian activity; however, the channel presented a fast aggradation and shrinkage state, mainly driven by low discharge and high incoming sediment coefficient. After 2005, water–sediment relations turned to a high discharge and low incoming sediment coefficient, combining to sharply weaken aeolian activities and riverbed rapid scouring rebound. However, the channel cross-section area and the talweg elevation revealed wandering and unstable desert channels.

Meanwhile, Wang et al. [48] indicated that the increase in perennial vegetation coverage, terrace farming and construction of check dams and reservoirs led to sediment load reduction. Moreover, the capacity of soil conservation and engineering measures to capture sediment will inevitably saturate over time. We must also pay attention to preventing a river sediment load rebound, which will probably induce channel aggradation in the Ulan Buh Desert reaches in the future.

5.4. Uncertainties and Limitations

In this desert reach of the upper Yellow River, channel changes are complex and are regulated by fluvial and aeolian processes. It is difficult to distinguish the contribution of each influencing factor, as lateral additions of aeolian sand are uncertain, and although some researchers have proposed some reference amounts for lateral additions of aeolian sand, these results are not fully mutually confirmed. Also, based on the cross-section and RS images, the estimations for channel scouring and deposition are not fully accurate. More surveying and monitoring devices need to operate in this area. However, these qualitative and semiquantitative results can help to reveal the mechanisms of desert rivers driven by aeolian and fluvial processes, tentatively, providing some reference for further attempts in future research.

6. Conclusions

In this paper, we present an outstanding example of how desert river channel evolution is regulated by aeolian–fluvial interactions in the Ulan Buh Desert of the Yellow River, based on a long-time series data set (1966–2019) of channel cross-sections. The results indicate that the lateral addition of aeolian sand, the water–sediment relationship and human interference have significant roles at different periods of channel evolution. Before 1986, higher discharge, lower sediment content and greater intensity of aeolian activity caused the aeolian–fluvial channel to maintain a relative scouring and silting balance with little human activity. From 1986 to 2000, increases in large reservoir operation, vegetation coverage and floodplain farming, coupled with water–sediment relationship variation, caused rapid deposition and shrinkage of the river channel. From 2000 to 2014, the channel maintained a slight scouring state. With the Haibowan reservoir beginning operation in 2014, the talweg rapidly underwent scouring and undercut rebound. However, an expanding and stable floodplain accelerated sedimentation on the floodplain and weakened river lateral erosion, indicating that the channel showed a shrinkage trend. Meanwhile, there were no significant changes in the periodical characteristics of the channel longitudinal erosion and deposition. On the whole, increasing human interference and decreasing wind dynamics have driven this desert wandering channel to shrink, to be stable and to gradually form a new balance of erosion and sedimentation.

Author Contributions: Conceptualization, X.J.; Data curation, H.W.; Funding acquisition, Y.L. and X.J.; Methodology, Y.L. and Q.M.; Visualization, Y.L. and J.W.; Writing—original draft, Y.L.; Writing—reviewing and editing, Y.L. and X.J. All authors have read and agreed to the published version of the manuscript.

Funding: This work was supported by the National Natural Science Foundation of China (Grant No. 42101016), the Special Fund of Inner Mongolia Autonomous Region for the Transformation of Scientific and Technological Achievements (Grant No. 2021CG0046), the High-level Innovative and Entrepreneurial Talent Introduction Program of Jiangsu Province (Grant No. (2020)31015) and Alxa League Science and Technology Plan Project (Grant No. AMYY 2021-19).

Data Availability Statement: The data in this study is confidential. Please contact the corresponding author if necessary.

Acknowledgments: We are grateful to the Yellow River Engineering and Management Bureau of the Inner Mongolia Autonomous Region for providing data support.

Conflicts of Interest: The authors declare no conflict of interest.

References

1. Leopold, L.B.; Wolman, M.G. River Channel Patterns: Braided, Meandering and Straight. *Prof. Geogr.* **1957**, *9*, 39–85.
2. Miall, A.D. A review of the braided-river depositional environment. *Earth-Sci. Rev.* **1977**, *13*, 1–62. [CrossRef]
3. Chang, H.H. Minimum stream power and river channel patterns. *J. Hydrol.* **1979**, *41*, 303–327. [CrossRef]
4. Schumm, S.A. Patterns of alluvial rivers. *Annu. Rev. Earth Planet. Sci.* **1985**, *13*, 5. [CrossRef]
5. Graf, W.L. Channel instability in a braided, sand bed river. *Water Resour. Res.* **1981**, *17*, 1087–1094. [CrossRef]
6. Lane, S.N.; Richards, K.S.; Chandler, J.H. Discharge and sediment supply controls on erosion and deposition in a dynamic alluvial channel. *Geomorphology* **1996**, *15*, 1–15. [CrossRef]
7. Bridge, J.S. The interaction between channel geometry, water flow, sediment transport and deposition in braided rivers. *Geol. Soc. Lond. Spec. Publ.* **1993**, *75*, 13–71. [CrossRef]
8. Frings, R.M. Downstream fining in large sand-bed rivers. *Earth-Sci. Rev.* **2008**, *87*, 39–60. [CrossRef]
9. Wang, S. Channel Pattern Specialities and the Formation of the Lower Reaches of the Yellow River. *Acta Geosicientia Sin.* **2003**, *24*, 73–78.
10. Chien, N. On the Classification and causes of formation of different channel patterns. *Acta Geogr. Sin.* **1985**, *40*, 1–10.
11. Lewin, J.; Brewer, P.A. Predicting channel patterns. *Geomorphology* **2001**, *40*, 329–339. [CrossRef]
12. Sarma, J.N. Fluvial process and morphology of the Brahmaputra River in Assam, India. *Geomorphology* **2005**, *70*, 226–256. [CrossRef]
13. Wang, S.; Fan, X. Flood Processes and Channel Responses in Typical Years of the Different Channel Patterns in Neimenggu Reaches of the Upper Yellow River. *Prog. Geogr.* **2010**, *29*, 565–571.
14. Schumm, S.A. A tentative classification of alluvial river channels. In Proceedings of the United States Geological Survey Circular, Millard County, UT, USA, 1 January 1963.
15. Sarker, M.H.; Thorne, C.R.; Aktar, M.N.; Ferdous, M.R. Morpho-dynamics of the Brahmaputra–Jamuna River, Bangladesh. *Geomorphology* **2014**, *215*, 45–59. [CrossRef]
16. Vitek, J.D. Geomorphology: Perspectives on observation, history, and the field tradition. *Geomorphology* **2013**, *200*, 20–33. [CrossRef]
17. Arfa-Fathollahkhani, A.; Ayyoubzadeh, S.A.; Shafizadeh-Moghadam, H.; Mianabadi, H. Spatiotemporal Characterization and Analysis of River Morphology Using Long-Term Landsat Imagery and Stream Power. *Water* **2022**, *14*, 3656. [CrossRef]
18. Schuurman, F.; Ta, W.; Post, S.; Sokolewicz, M.; Busnelli, M.; Kleinhans, M. Response of braiding channel morphodynamics to peak discharge changes in the Upper Yellow River. *Earth Surf. Process. Landf.* **2018**, *43*, 1648–1662. [CrossRef]
19. Dissanayake, D.; Roelvink, J. *Effect of Sediment Transport Formulation on Long-Term Morphology*; European Geophysical Union (EGU): Vienna, Austria, 2008.
20. Li, J. *Development Environment and Evolution Patterns of Linear Dunes in the Qaidam Basin*; Xi'an Jiaotong University Press: Xi'an, China, 2020.
21. Davis, W.M. The geographical cycle. *Geogr. J.* **1899**, *14*, 481–504. [CrossRef]
22. Bagnold, R.A. The Movement of Desert Sand. *Geogr. J.* **1936**, *157*, 342–365. [CrossRef]
23. Tooth, S. Process, form and change in dryland rivers: A review of recent research. *Earth-Sci. Rev.* **2000**, *51*, 67–107. [CrossRef]
24. Yang, H.; Shi, C. Spatial and temporal variations of aeolian sediment input to the tributaries (the Ten Kongduis) of the upper Yellow River. *Aeolian Res.* **2018**, *30*, 1–10. [CrossRef]
25. Al-Masrahy, M.A.; Mountney, N.P. A classification scheme for fluvial-aeolian system interaction in desert-margin settings. *Aeolian Res.* **2015**, *17*, 67–88. [CrossRef]
26. Belnap, J.; Munson, S.M.; Field, J.P. Aeolian and fluvial processes in dryland regions: The need for integrated studies. *Ecohydrology* **2011**, *4*, 615–622. [CrossRef]
27. Liu, B.; Coulthard, T.J. Mapping the interactions between rivers and sand dunes: Implications for fluvial and aeolian geomorphology. *Geomorphology* **2015**, *231*, 246–257. [CrossRef]

28. Breshears, D.D.; Whicker, J.J.; Johansen, M.P.; Pinder, J.E. Wind and water erosion and transport in semi-arid shrubland, grassland and forest ecosystems: Quantifying dominance of horizontal wind-driven transport. *Earth Surf. Process. Landf.* **2003**, *28*, 1189–1209. [CrossRef]
29. Bullard, J.E.; McTainsh, G.H. Aeolian-fluvial interactions in dryland environments: Examples, concepts and Australia case study. *Prog. Phys. Geogr.* **2003**, *27*, 471–501. [CrossRef]
30. Field, J.P.; Breshears, D.D.; Whicker, J.J. Toward a more holistic perspective of soil erosion: Why aeolian research needs to explicitly consider fluvial processes and interactions. *Aeolian Res.* **2009**, *1*, 9–17. [CrossRef]
31. Langford, R.P. Fluvial-aeolian interactions: Part I, modern systems. *Sedimentology* **2010**, *36*, 1023–1035. [CrossRef]
32. Ta, W.; Wang, H.; Jia, X. Downstream fining in contrasting reaches of the sand-bedded Yellow River. *Hydrol. Process.* **2011**, *25*, 3693–3700. [CrossRef]
33. Smith, N.D.; Smith, D.G. William River: An outstanding example of channel widening and braiding caused by bed-load addition. *Geology* **1984**, *12*, 78–82. [CrossRef]
34. Li, S.; Dong, G.; Shen, J.; Yang, P.; Liu, X.; Wang, Y.; Jin, H.; Wang, Q. Formation mechanism and development pattern of aeolian sand landform in Yarlung Zangbo River valley. *Sci. Sin. Terrae* **1999**, *42*, 272–284. [CrossRef]
35. Li, Y.; Wang, H.; Ma, Q. Responses of the Braided Channel to Reduced Discharge and Lateral Inputs of Aeolian Sand in the Ulan Buh Desert Reach of the Upper Yellow River. *Environ. Earth Sci.* **2018**, *77*, 379. [CrossRef]
36. Jia, X.; Wang, H.; Li, Y. Desert channel erosion, accretion characteristics and their implications for aeolian–fluvial interactions: A case study in a desert watershed in the Ordos Plateau, China. *Environ. Earth Sci.* **2021**, *80*, 371. [CrossRef]
37. Wang, H.; Jia, X.; Li, Y.; Peng, W. Selective deposition response to aeolian–fluvial sediment supply in the desert braided channel of the upper Yellow River, China. *Nat. Hazards Earth Syst. Sci.* **2015**, *15*, 1955–1962. [CrossRef]
38. Yang, G.; Ta, W.; Dai, F.; Liu, Y.; Jing, K.; Li, B.; Zhang, O.; Lu, R.; Hu, L.; Tao, Y. Contribution of Sand Sources to the Silting of Riverbed in Inner Mongolia Section of Huanghe River. *J. Desert Res.* **2003**, *23*, 54–61.
39. Jia, X.; Wang, H.; Xiao, J. Geochemical elements characteristics and sources of the riverbed sediment in the yellow river's desert channel. *Environ. Earth Sci.* **2011**, *64*, 2159–2173. [CrossRef]
40. Pang, H.; Pan, B.; Garzanti, E.; Gao, H.; Zhao, X.; Chen, D. Mineralogy and geochemistry of modern Yellow River sediments: Implications for weathering and provenance. *Chem. Geol.* **2018**, *488*, 76–86. [CrossRef]
41. Yang, G. *Symposia on Blown-Sand Disaster*; Ocean Press: Beijing, China, 2005. (In Chinese)
42. Xu, X. China annual vegetation index (NDVI) spatial distribution data set. In *Registration and Publication System of Resources and Environmental Science Data*; Chinese Academy of Sciences: Beijing, China, 2018. [CrossRef]
43. Mann, H.B. Nonparametric test against trend. *Econometrica* **1945**, *13*, 245–259. [CrossRef]
44. Kendall, M.G. *Rank Correlation Methods*; APA: Camberwell, Australia, 1975.
45. Percival, D.B.; Walden, A.T. *Wavelet Methods for Time Series Analysis*; Cambridge University Press: Cambridge, UK, 2000.
46. Kasai, M.; Marutani, T.; Brierley, G. Channel bed adjustments following major aggradation in a steep headwater setting: Findings from Oyabu Creek, Kyushu, Japan. *Geomorphology* **2004**, *62*, 199–215. [CrossRef]
47. Ta, W.; Xiao, H.; Dong, Z. Long-term morphodynamic changes of a desert reach of the Yellow River following upstream large reservoirs' operation. *Geomorphology* **2008**, *97*, 249–259. [CrossRef]
48. Wang, S.; Fu, B.; Piao, S.; Lu, Y.; Ciais, P.; Feng, X.; Wang, Y. Reduced sediment transport in the Yellow River due to anthropogenic changes. *Nat. Geosci.* **2015**, *9*, 38–41. [CrossRef]